the plant journal

SEB SOCIETY FOR EXPERIMENTAL BIOLOGY

The Plant Journal (2024) **118,** 58–72 doi: 10.1111/tpj.16589

Verbascum species as a new source of saffron apocarotenoids and molecular tools for the biotechnological production of crocins and picrocrocin

Lucía Morote[1], Ángela Rubio-Moraga[1,2], Alberto José López Jiménez[1,2], Verónica Aragonés[3], Gianfranco Diretto[4], Olivia Costantina Demurtas[4], Sarah Frusciante[4], Oussama Ahrazem[1,2], José-Antonio Daròs[3] and Lourdes Gómez-Gómez[1,5,*]

[1]*Instituto Botánico, Departamento de Ciencia y Tecnología Agroforestal y Genética, Universidad de Castilla-La Mancha, Campus Universitario s/n, 02071 Albacete, Spain,*

[2]*Escuela Técnica Superior de Ingeniería Agronómica y de Montes y Biotecnología. Departamento de Ciencia y Tecnología Agroforestal y Genética, Universidad de Castilla-La Mancha, Campus Universitario s/n, 02071 Albacete, Spain,*

[3]*Instituto de Biología Molecular y Celular de Plantas (Consejo Superior de Investigaciones Científicas-Universitat Politècnica de València), 46022,Valencia, Spain,*

[4]*Italian National Agency for New Technologies, Energy, and Sustainable Development, Casaccia Research Centre, 00123 Rome, Italy, and*

[5]*Facultad de Farmacia, Universidad de Castilla-La Mancha, Campus Universitario s/n, 02071 Albacete, Spain*

Received 17 July 2023; revised 27 November 2023; accepted 4 December 2023; published online 15 December 2023.
*For correspondence (e-mail marialourdes.gomez@uclm.es).
[Correction added on 09 January 2024, after first online publication: The name of the sixth author has been corrected to Olivia Costantina Demurtas in this version.]

SUMMARY

Crocins are glucosylated apocarotenoids present in flowers and fruits of a few plant species, including saffron, gardenia, and *Buddleja*. The biosynthesis of crocins in these plants has been unraveled, and the enzymes engineered for the production of crocins in heterologous systems. Mullein (*Verbascum* sp.) has been identified as a new source of crocins and picrocrocin. In this work, we have identified eight enzymes involved in the cleavage of carotenoids in two *Verbascum* species, *V. giganteum* and *V. sinuatum*. Four of them were homologous to the previously identified BdCCD4.1 and BdCCD4.3 from *Buddleja*, involved in the biosynthesis of crocins. These enzymes were analyzed for apocarotenogenic activity in bacteria and *Nicotiana benthamiana* plants using a virus-driven system. Metabolic analyses of bacterial extracts and *N. benthamiana* leaves showed the efficient activity of these enzymes to produce crocins using β-carotene and zeaxanthin as substrates. Accumulations of 0.17% of crocins in *N. benthamiana* dry leaves were reached in only 2 weeks using a recombinant virus expressing VgCCD4.1, similar to the amounts previously produced using the canonical saffron CsCCD2L. The identification of these enzymes, which display a particularly broad substrate spectrum, opens new avenues for apocarotenoid biotechnological production.

Keywords: crocetin, carotenoid cleavage dioxygenase, *Buddleja*, crocus, *Verbascum*, metabolic engineering.

INTRODUCTION

Carotenoids are tetraterpenoid polyenes produced in plants, microbes, and by certain aphids and spider mites (Maoka, 2021). In plants, carotenoid biosynthesis starts with phytoene production, a colorless carotenoid with three conjugated double bonds, and continues with sequential reactions of desaturation and isomerization, which lead to the formation of all-*trans*-lycopene. Lycopene cyclase activities give rise to various carotenes including δ-carotene, ε-carotene, α-carotene, and β-carotene; further oxygenation of these cyclized carotenes produces a series of xanthophylls, including lutein, zeaxanthin, antheraxanthin, violaxanthin, and neoxanthin (Rodriguez-Concepcion et al., 2018). Carotenoid complexity is further increased by additional transformations, including isomerizations, oxidations, and the enzymatic cleavage of the polyene chain. This last reaction is catalyzed by a family of enzymes named carotenoid cleavage dioxygenases (CCDs), which cleave carotenoids at their double bonds (Auldridge, McCarty, & Klee, 2006). The first CCD was identified in the Viviparous 14 (Vp14) mutant of

maize and is involved in the biosynthesis of abscisic acid (ABA) (Schwartz et al., 1997). The identification of Vp14 further allowed the identification of other CCDs in animals and plants (Ahrazem, Gomez-Gomez, et al., 2016). Nine-cis epoxycarotenoid dioxygenases (NCEDs; NCED2, NCED3, NCED5, NCED6, and NCED9) are all CCD enzymes that, like Vp14, are involved in ABA biosynthesis. NCEDs recognize and cleave the 11,12;11′,12′ double bond of 9-*cis*-violaxanthin or 9-*cis*-neoxanthin (Schwartz et al., 2003). All other CCDs that are not involved in the production of ABA are categorized as CCDs. There are many CCD subfamilies, and genome sequencing is contributing to the discovery of new ones. In particular, six CCDs, including CCD1, CCD2, CCD4, CCD7, CCD8, and ZAX (CCD10), have divergent cleavage properties and locations in the cell (Alder et al., 2008; Auldridge, Block, et al., 2006; Frusciante et al., 2014; Ilg et al., 2014; Rubio et al., 2008; Rubio-Moraga et al., 2014). More specifically, CCD1 coding genes have been found in all the plant genomes studied so far (https://phytozome.jgi.doe.gov); the enzymes of this subfamily recognize and cleave a wide range of carotenoids at different positions (Garcia-Limones et al., 2008; Huang et al., 2009; Ibdah et al., 2006; Ilg et al., 2014; Schmidt et al., 2006; Simkin et al., 2004), and, for this reason, their activities have been proposed to be associated to apocarotenoid degradation (Simkin, 2021). CCD2, closely related to CCD1, but with plastid localization, drives zeaxanthin catabolism at positions 7,8;7′,8′ in *Crocus* species, yielding crocetin-dialdehyde (Ahrazem, Rubio-Moraga, et al., 2016; Frusciante et al., 2014), further transformed into crocins (Gomez-Gomez et al., 2017, 2018; López-Jimenez et al., 2021; Moraga et al., 2004). Besides CCD2, in the CCD4 subfamily, specific chromoplastic localized CCD4 enzymes from *Buddleja davidii* and gardenia act on carotenoids at positions 7,8;7′,8′ to generate crocins as well (Ahrazem et al., 2017; Xu et al., 2020; Zheng et al., 2022). Other enzymes in this subfamily only recognize the 7,8 or 7′,8′ position, leading to the formation of β-citraurin (Ma et al., 2013; Rodrigo et al., 2013). Inside this subfamily, other CCD4 enzymes with a plastoglobuli localization are involved in the generation of aroma volatiles (Morote et al., 2023; Rubio et al., 2008; Wang et al., 2020), catalyzing the cleavage of 9,10;9′,10′ double bonds. However, these enzymes are also responsible for the degradation of carotenoids in different tissues and the loss of coloration of fruits and flowers (Awasthi et al., 2022; Brandi et al., 2011; Bruno et al., 2015; Gonzalez-Jorge et al., 2013; Morote et al., 2023; Ohmiya et al., 2006; Zhang et al., 2015, 2023). Carotenoids, in particular β-carotene, can be sequentially cleaved by the activities of plastidic CCD7 (at positions 9,10 or 9′,10′) and CCD8 (at positions 13,14), resulting in carlactone as the precursor to strigolactone (Alder et al., 2008, 2012). More recently, a novel CCD subfamily has been characterized, zaxinone synthase (ZAS), which cleaves apo-10′-zeaxanthinal at the 13,14 double bond to produce zaxinone in rice (Wang et al., 2019), and the homologous enzymes have been designated as the CCD10 subfamily (Zhong et al., 2020).

Verbascum is a widespread genus of the family *Scrophulariaceae*, which comprises 300 to 325 Euro Asiatic species. It is the largest genus of the family, whose origin has been traced to the center of the Eastern Mediterranean basin (Benedí, 2009). Some species from this genus has been traditionally used to treat a variety of disorders, such as asthma, spasmodic coughs, inflammatory illnesses, diarrhea, migraine headaches, and malaria (Jan et al., 2022). Although these species have been used in traditional medicine since antiquity, their commercial appeal has grown recently, and this growth is being backed up by an increasing number of research studies (Blanco-Salas et al., 2021). Many secondary metabolites, belonging to different biosynthetic pathways (terpenoids, shikimic acid derivatives, and mixed metabolites), have been detected in a few *Verbascum* species, such as *V. cheiranthifolium* Boiss., *V. lychnitis* L., *V. songaricum* Schrenk, *V. speciosum* Schrad. and *V. thapsus* L. In particular, by using different color reactions, it was determined that crocin was one of the pigments responsible for the yellow color of the petals of the flowers of *V. thapsus* L. (Bate-Smith, 1953).

Crocins are one of the three main metabolites present in the stigmas of *Crocus sativus* (Pfander & Schurtenberger, 1982). These secondary metabolites are crocetin esters with a variable number of sugar molecules attached to the ends of the apocarotenoid, which confer variable solubility to the compounds. Crocins are responsible for the pigmentation of the saffron spice and, besides providing color, they exhibit a number of beneficial pharmacological effects due to their anti-inflammatory and anti-oxidative properties (Salih *et al.*, 2019). Therefore, these valuable pigments are used across multiple commercial sectors such as the food and health supplement industries. Crocetin is generated in *Crocus* species by the action of CCD2 using zeaxanthin as substrate (Ahrazem, Rubio-Moraga, et al., 2016; Frusciante et al., 2014), and in *B. davidii* two CCD4 enzymes, BdCCD4.1 and BdCCD4.3, catalyzed the same reaction (Ahrazem et al., 2017). *B. davidii* also belongs to the family *Scrophulariaceae* and is closely related to *Verbascum* (Dong et al., 2022). Therefore, we expected to identify the homologous enzymes responsible for crocetin biosynthesis in *Verbascum*. In this work, we evaluated the presence and nature of crocins in the yellow flowers from two *Verbascum* species, *V. giganteum* and *V. sinuatum*. The first species can be found in limestone mountain peaks, where it grows on slopes, stony slopes, and short herbaceous meadows in valleys. It is endemic to the southern half of the Iberian Peninsula. The second species is a ruderal plant, which grows on nitrified and altered land, such as roadsides and old fallow land, and has a broad distribution in the Iberian Peninsula (http://www.floraiberica.es/). We identified and isolated four *CCD* genes in each species, including a *CCD1* homolog and three genes related to the *CCD4* subfamily. One of the *CCD4*

genes was highly expressed in the tepals and was found to cleave β-carotene and zeaxanthin at 7,8;7′,8′ double bonds to efficiently produce crocetin dialdehyde. Overall, this study provides with novel CCD4 enzymes that can be used as biotechnological tools to drive crocin biosynthesis in different heterologous systems.

RESULTS

Crocins in flowers of *Verbascum* species

Flowers of *V. giganteum* and *V. sinuatum* showed five yellow petals and five stamens (Figure 1). Open flowers were analyzed for the accumulation of picrocrocin and crocins and compared with saffron stigmas (Figure 2a,b). Picrocrocin and HTCC were detected in the petals of both species (Figure 2a). Notably, picrocrocin with gentiobiose was present at higher proportion in *V. sinuatum* (70% from the total picrocrocin derivatives), while the canonical picrocrocin molecule was predominant in *V. giganteum* (58% of the total picrocrocin derivatives) (Figure 2a). The crocins that accumulate in saffron were also present at high levels in *V. sinuatum* and *V. giganteum* as trans-crocetin-di-(β-D-gentiobiosyl)-ester (t-3Gg), trans-(crocetin-(β-D-gentiobiosyl)-(β-D-glucosyl)-ester (t-4GG), trans-crocetin-di-(β-D-glucosyl)-ester (t-2gg) and cis-crocetin-(β-D-glucosyl)-ester (c-1 g). Although, crocins with 6 and 5 glucose molecules were also identified (Figure S1a and Table S1), compared with saffron, crocin with 6 glucose molecules was more abundant in *Verbascum* than in saffron, especially in *V. giganteum*. We also compared the pattern observed for both *Verbascum* species with that from *B. davidii* petals (Figure S1b). Interestingly, the crocin patterns were very similar. Crocins concentration was determined in closed flowers and in open flowers. The concentration of crocins in open flowers was higher than in closed flowers in both species. In closed flowers of *V. giganteum*, crocins accumulated at 7.6 ± 1.1 mg/g dry weight (DW) and in open flowers at 9.87 ± 1.7 mg/g DW. In *V. sinuatum*, the obtained levels of crocins were 11.03 ± 1.7 and 14.38 ± 2.6 mg/g DW in closed and open flowers, respectively. We further determined the presence of carotenoids in the open flowers in both species and observed the accumulation of lutein, zeaxanthin, and β-carotene as common carotenoids in both species (Figure 2c; Figure S2). More specifically, β-carotene was detected as the main carotenoid present in both flowers, although the highest levels were reached in *V. sinuatum* (Figure 2c).

Identification of carotenoids cleavage dioxygenases in *Verbascum*

Two previously obtained transcriptomes from flowers of *V. giganteum* and *V. sinuatum* were compared to *B. davidii* CCD enzymes using BLAST analyses. The search resulted in the identification of different contigs for a total of four *CCD* sequences in each species, including homologs to

Figure 1. Images of *Verbascum sinuatum* and *V. giganteum* used in this study. In the left side are shown the inflorescences and in the right side are shown the plants in the flowering stage.

CCD1, *CCD4.1*, *CCD4.2*, and *CCD4.3* (Table 1). Maximum similarities were found with the CCD enzymes of *B. davidii* (Table 1). The sequences were also analyzed for N-terminal targeting signals. The CCD1 enzymes were predicted to be targeted to the cytosol, and CCD4.1, CCD4.2, and CCD4.3 were all predicted to have an N-terminal transit peptide for plastids targeting (Table 1). All the characterized CCD enzymes showed the four highly conserved His residues involved in the coordination of the non-heme Fe II prosthetic group (Kloer & Schulz, 2006) (Figure S3).

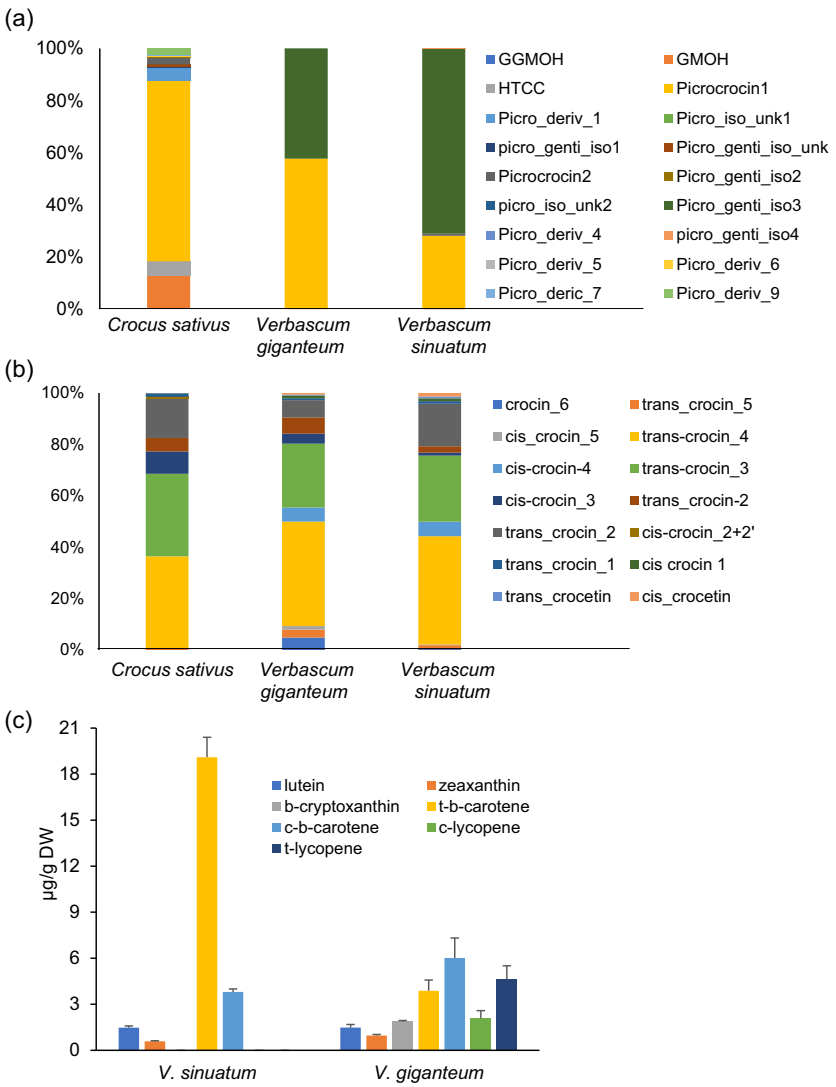

Figure 2. Apocarotenoid and carotenoid content and composition in polar extracts of petals of *Verbascum* species.
(a) Levels of picrocrocin derivatives and HTCC.
(b) Crocetin, and crocin accumulation.
(c) Carotenoid levels in both species. Columns represent the mean and SD of three biological replicates, each including three technical replicates.

Multiple sequence alignment analysis of CCDs from different plant species, retrieved from databases, and their phylogeny along with the sequences from both *Verbascum* species, exhibit closeness to *B. davidii* enzymes. The CCD1 proteins of both *Verbascum* species fall into the CCD1 subfamily found in other plants (Figure 3); similarly, CCD4.2 enzymes belong to the CCD4 subfamily from dicotyledonous plants (Figure 4). CCD4.1 and CCD4.3, on the other hand, constitute a distinct cluster containing *Buddleja* enzymes that is sister to the main CCD4 group (Figure 3), which mostly includes enzymes involved in floral and fruit color loss and flower aroma (Brandi et al., 2011; Ohmiya et al., 2006).

Changes in the expression of CCD4 genes in *Verbascum* species

To understand whether and how crocins contents are transcriptionally regulated in *V. sinuatum* and *V. giganteum*, we used qPCR to analyze the expression levels of all identified *CCD* genes in the petal tissues in closed and open flowers of both species. In comparison to the expression levels of all the other *CCDs*, *CCD4.1* had the highest levels of expression in both the pre-anthesis and anthesis stages in *V. sinuatum* and *V. giganteum* (Figure 4a). In *V. sinuatum*, the levels of expression of *CCD1* were higher than those of *CCD4.2* and *CCD4.3* (Figure 4a), whereas in *V.*

Table 1 Characteristics of *Verbascum* CCDs. Vs refers to *V. sinuatum*, while Vg refers to CCDs from *V. giganteum*

Name and GenBank accession number	aa	MW/PI	Identity %	Predicted location
VsCCD1, OR037091	543	61.40/6.40	93.48% APU54678.1 (*B. davidii*)	Cytosol
VgCCD1, OR037087	540	61.30/6.27	94.61% APU54678.1 (*B. davidii*)	Cytosol
VsCCD4.1, OR037089	572	63.98/8.21	76.22% APU54674.1 (*B. davidii*)	Plastid
VgCCD4.1, OR037085	572	64.15/6.48	76.0% APU54674.1 (*B. davidii*)	Plastid
VsCCD4.2, OR037090	574	62.68/7.70	86.14% APU54675.1 (*B. davidii*)	Plastid
VgCCD4.2, OR037086	590	64.22/8.42	85.09% APU54675.1 (*B. davidii*)	Plastid
VsCCD4.3, OR037088	583	64.73/6.93	75.17% APU54676.1 (*B. davidii*)	Plastid
VgCCD4.3, OR037084	530	58.81/6.11	77.85% APU54676.1 (*B. davidii*)	Plastid

giganteum the levels of expression of *CCD4.2* were higher than those of *CCD1* and *CCD4.3* (Figure 4a). The transcript levels of *CCD4.3* were the lowest in the two developmental stages in both species (Figure 4a).

Furthermore, the expression levels of selected genes related to the carotenoid biosynthetic pathway were analyzed (Figure 4b). More in detail, the expression levels of *PSY1*, *B-LCY-1*, *Lut1*, and *Lut5* were low in all the samples (Figure 4b), compared to the expression levels of the other carotenogenic genes. In both species, *PSY2*, *PDS*, *ZDS*, *Z-ISO*, *CRTISO*, and *B-LYC-2* showed higher levels of expression in anthesis (Figure 4b). However, the expression of *BCH* increased at anthesis in *V. sinuatum* and decreased in *V. giganteum* (Figure 4b). Despite this, the transcript levels of *BCH* showed the highest levels of expression in pre-anthesis and anthesis petals in both species. In addition, the transcript levels of *Or* were examined. Of interest, *V. giganteum* had low levels of expression in the tepals, whereas *V. sinuatum* petals had a high level of expression (Figure 4b). This high level of *Or* expression in *V. sinuatum* may be related to the higher levels of β-carotene in the petals (Figure 2c).

Functional analyses of recombinant CCD4.1 proteins

Due to the high expression levels of these *CCD4.1* genes and their relationships with the accumulation of crocins. VgCCD4.1 was selected to examine *in vivo* activity in *E. coli* as well as in *N. benthamiana* plants; notably this enzyme is 95.1% identical to VsCCD4.1 (Figure S4). Lycopene, β-carotene, and zeaxanthin were used as substrates to assay the enzymatic activity of VgCCD4.1 *in vivo* in *E. coli*. While for the assay of VgCCD4.1 in *N. benthamiana*, a previously developed virus-driven system to produce crocins was used (Martí et al., 2020). For the assays in *E. coli*, the full-length cDNA, excluding the first amino acids predicted to be the transit peptide for plastid localization, was cloned into the expression vector pThio-Dan1 (Bruno et al., 2014), and the recombinant plasmid was introduced in *E. coli* cells that produced and accumulated different carotenoid substrates. The reaction products were characterized by GC–MS and HPLC-DAD-HRMS. The volatile β-cyclocitral was detected in the headspace of β-carotene-producing *E. coli* cells expressing the VgCCD4.1 protein (Figure 5). In zeaxanthin-producing cells expressing VgCCD4.1, a volatile was identified as HTCC (Figure 5). β-cyclocitral and HTCC have generated as a result of a 7,8;7′8′ cleavage activity on β-carotene and zeaxanthin, respectively. Therefore, the obtained results suggested that β-carotene and zeaxanthin were recognized as substrates of VgCCD4.1, which catalyzed the cleavage at the 7,8;7′8′ double bonds. However, we did not detect any additional peak for the cultures of bacterial cells that accumulate lycopene when the expression of VgCCD4.1 was induced, suggesting that lycopene was not a substrate for this enzyme. Furthermore, to identify the non-volatile apocarotenoids produced by the activity of VgCCD4.1, the pigments produced by carotenoid-accumulating *E. coli* expressing VgCCD4.1 were analyzed by HPLC. Compared with the empty vector, the UV/Vis absorbance spectrum obtained from the β-carotene and zeaxanthin background from bacterial cells expressing VgCCD4.1 showed a peak that matched crocetin dialdehyde based on UV/Vis spectrum and retention time (Figure 6). Crocetin dialdehyde was confirmed by MS analyses (Figure 6). On the contrary, we could not detect any additional peak for the cultures of cells that accumulate lycopene when the expression of VgCCD4.1 was induced, suggesting that lycopene was not a substrate for this enzyme.

Subsequently, we constructed a recombinant virus (Figure 7a) to express VgCCD4.1 (TEV-VgCCD4.1) in *N. benthamiana*. VgCCD4.1 is a plastidic enzyme that must contain the native amino-terminal transit peptide. Thus, to target the enzyme to the plastids, we inserted the cDNA in a position in the virus genome that corresponds to the amino terminus of the viral polyprotein (Martí et al., 2020). In addition, *VgCCD4.1* cDNA also contained, at the 3′ end, a sequence for an artificial NIaPro cleavage site to allow the release of the heterologous protein from the viral polyprotein. Based on previous work, we used the −8/+3 site, which splits NIb and CP in TEV. The obtained recombinant clon was agroinoculated in *N. benthamiana* plants. As a control, some plants were agroinoculated with TEV-aGFP which expresses GFP located at the most amino-terminal position in the viral polyprotein. Symptoms of infection

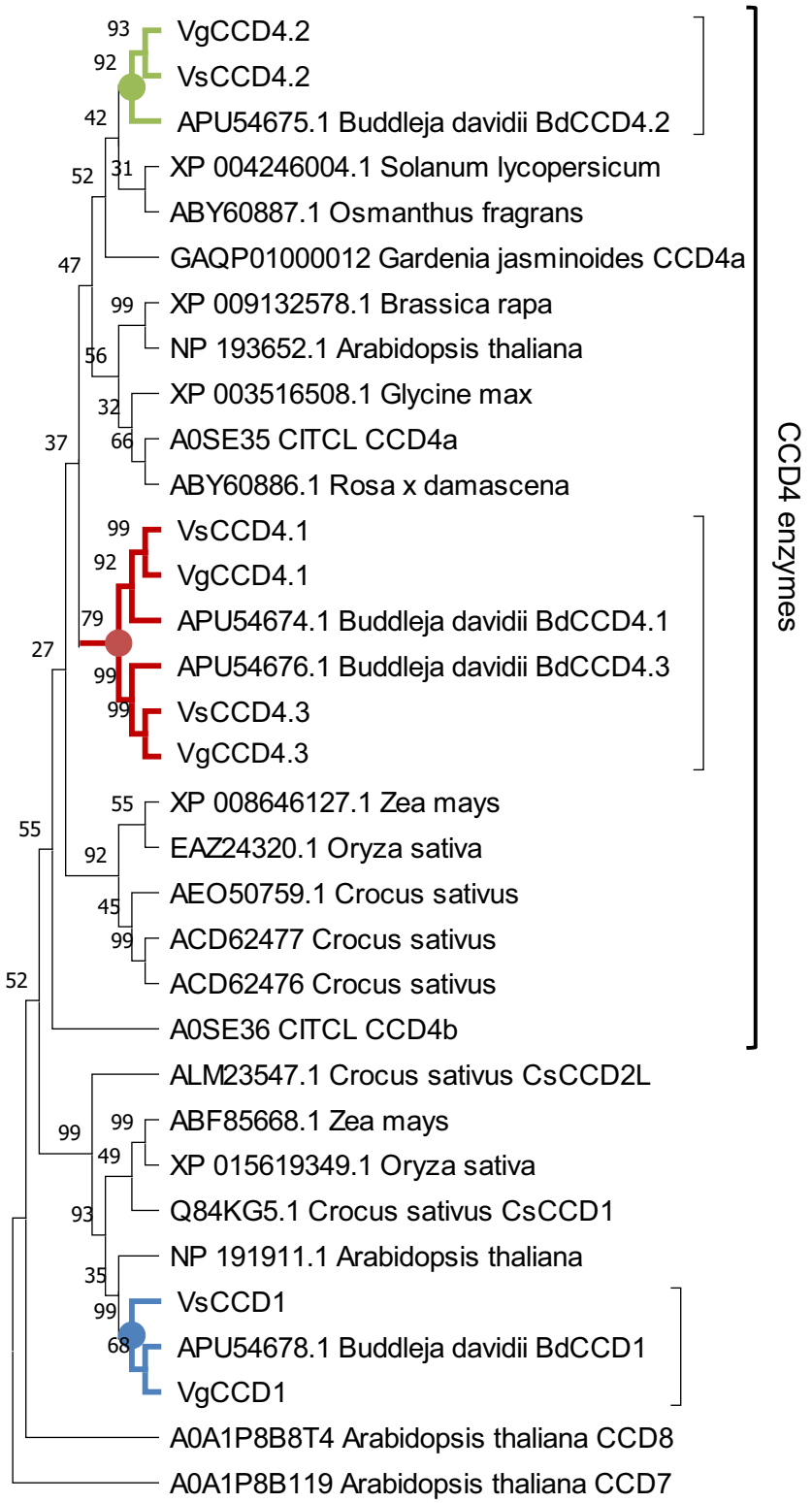

Figure 3. The evolutionary history of selected CCDs was inferred using the Minimum Evolution method. The optimal tree is shown. The percentage of replicate trees in which the associated taxa clustered together in the bootstrap test (5000 replicates) are shown above the branches. The evolutionary distances were computed using the Poisson correction method and are in the units of the number of amino acid substitutions per site. Evolutionary analyses were conducted in MEGA11 (https://megasoftware.net/). Branches including *Verbascum sp.* CCDs are highlighted in blue (CCD1), green (CCD4.2), and red (CCD4.3).

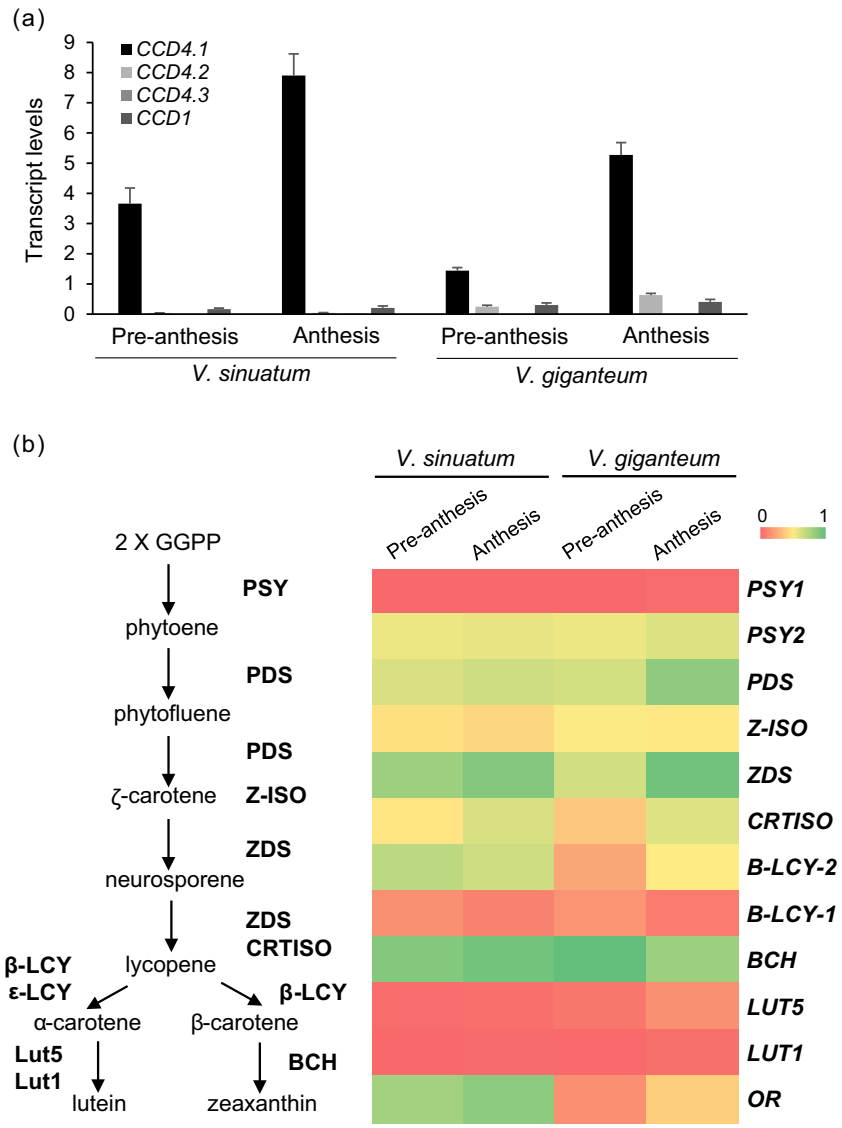

Figure 4. Quantitative expression analyses of the transcripts levels of genes involved in carotenoid biosynthesis and cleavage by RT-qPCR in petals at two developmental stages of *V. sinuatum* and *V. giganteum*.
(a) Expression levels of *CCD* genes in petals at pre-anthesis and anthesis of flowers of *V. giganteum* and *V. sinuatum*. Values are means ±SD.
(b) Representation of the main steps of the carotenoid biosynthetic pathway and heat map analysis showing gene expression pattern in pre-anthesis and anthesis petals of flowers of *V. giganteum* and *V. sinuatum*. Color from red to green indicates low to high expression.

were observed at approximately 8 dpi in plants agroinoculated with TEV-VgCCD4.1, and TEV-aGFP. A distinctive yellow pigmentation was observed in tissues of plants agroinoculated with TEV-VgCCD4.1 at approximately 14 dpi (Figure 7b). Symptomatic leaves from plants infected with TEV-aGFP and TEV-VgCCD4.1 were subjected to extraction and analysis to determine their crocins and carotenoid profiles. Analysis of the polar metabolic fraction of tissues infected with TEV-VgCCD4.1 showed a series of peaks with maximum absorbance around 440 nm, corresponding to crocins with different degrees of glucosylation, as revealed by HPLC-HRMS (Figure 7c). These peaks were not observed in the counterpart extracts from tissues from mock-inoculated plants or plants infected with the TEV-aGFP control. Predominant crocins were those conjugated with three and two glucose molecules. Subsequently, the levels of carotenoids and chlorophylls in the apolar fractions were also investigated (Figure S5). The comparison between tissues infected with TEV-aGFP and TEV-VgCCD4.1 showed differences in metabolite level in both carotenoids and chlorophylls. Chlorophyll and pheophytin were all reduced in TEV-VgCCD4.1. At the carotenoid level, the most striking differences were in the contents of phytoene and β-carotene, which were strongly

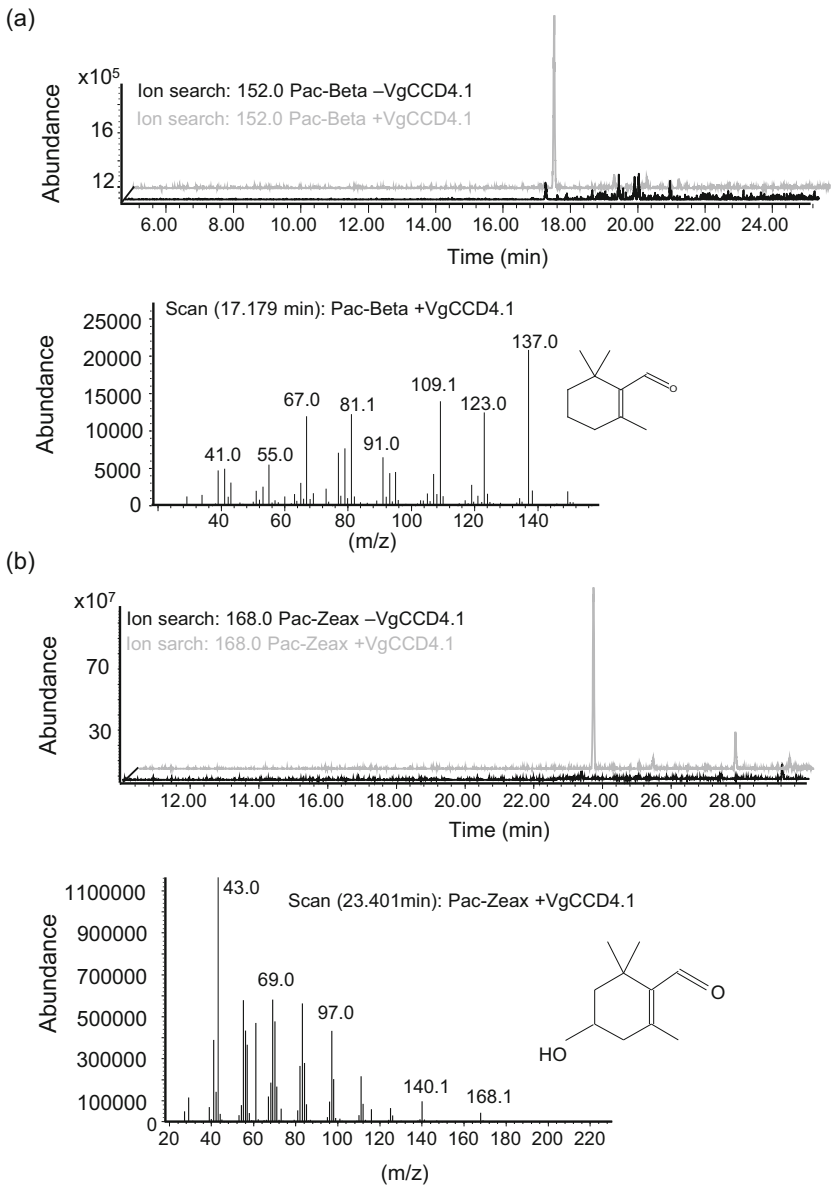

Figure 5. Chromatograms obtained from SHHE-GC–MS analyses of VgCCD4.1 activity in *E. coli* cells producing different carotenoid substrates.
(a) Control (black) and β-carotene-producing *E. coli* culture expressing VgCCD4.1 (gray) and β-cyclocitral MS spectrum (bottom). The retention time and mass spectra of the peak at 17.17 min from the VgCCD4.i-expressing *E. coli* were identical to those of β-cyclocitral.
(b) Chromatograms obtained from SHHE-GC–MS analysis of control zeaxanthin-producing *E. coli* cells (black) and zeaxanthin-producing *E. coli* culture expressing VgCCD4.1 (gray). The mass spectra and retention time of the peak at 23.40 min upon VgCCD4.1 expression were identical to HTCC.

reduced in TEV-VgCCD4.1-infected leaves (Figure S5), which further reinforced the additional activity of this enzyme in targeting β-carotene. Overall, this experiment revealed a remarkable accumulation of 1.78 ± 0.13 mg of crocins per gram of *N. benthamiana* DW leaf tissue.

In silico comparison among BdCCD4.1, VgCCD4.1, VsCCD4.1 and other CCDs

Phylogenetic analyses showed that BdCCD4.1, VgCCD4.1, and VsCCD4.1 clustered together, finding of particular interest given that BdCCD4.1 and *Verbascum* CCD4.1 proteins showed the same activity. Despite the fact that *Verbascum* enzymes have broader substrate specificity, we chose to investigate the structure of these enzymes to better understand this difference in specificity. First, the tridimensional structures of VgCCD4.1 and VsCCD4.1 enzymes were overlapped (Figure S6a), and then, overlapped with BdCCD4.1 (Figure S6b). In general, the tridimensional structures of the three enzymes were well conserved, although some differences were found

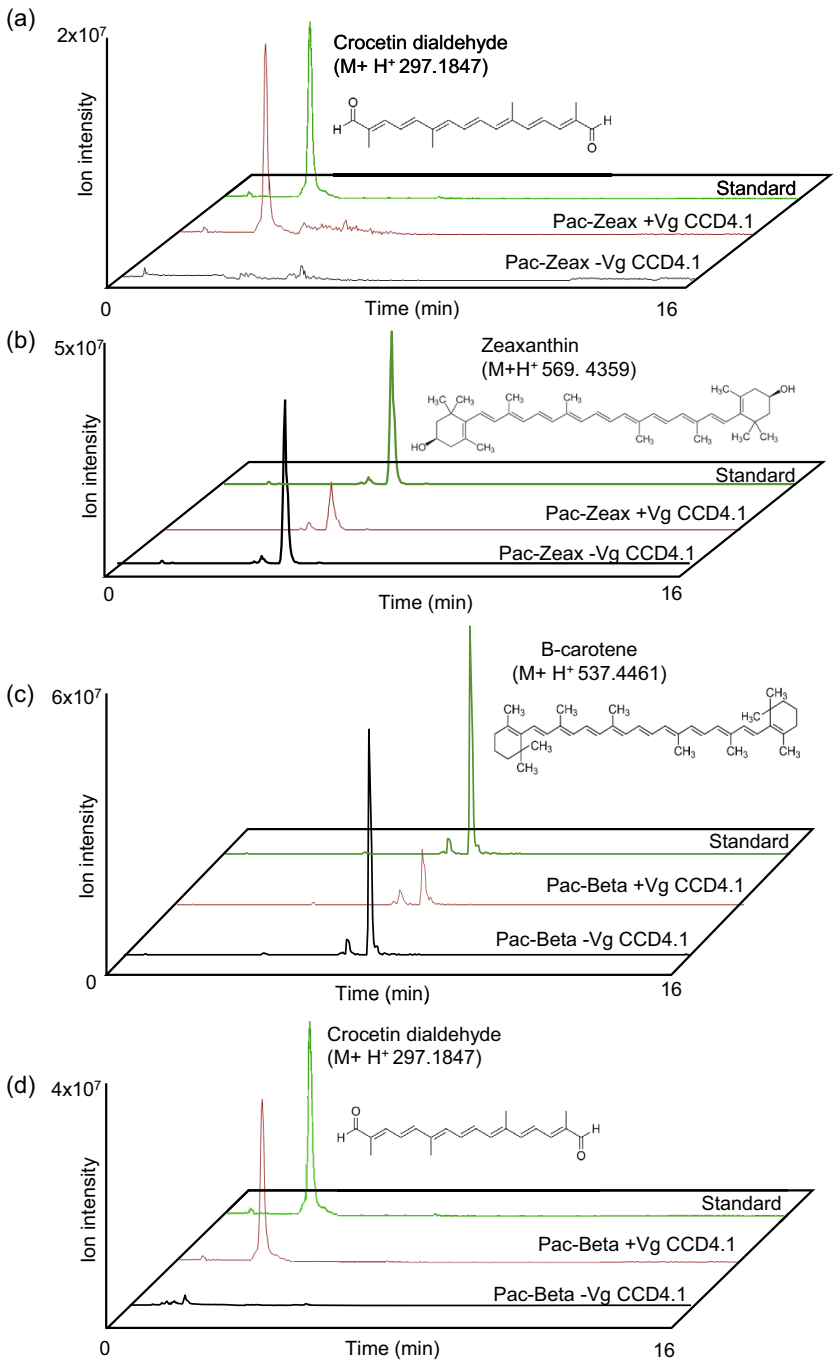

Figure 6. Chromatograms obtained by HPLC-DAD-HRMS of the *in vivo* assays in bacteria of VgCCD4.1.
(a) Induction of VgCCD4.1-expressing *E. coli* cells converted zeaxanthin into crocetin dialdehyde, as detected by HPLC-MS system alongside authentical standard for the confirmation of the identity of the cleavage product.
(b) Induction of VgCCD4.1-expressing *E. coli* cells converted zeaxanthin into crocetin dialdehyde, as detected by a reduction of zeaxanthin as substrate by HPLC-MS system.
(c) Induction of VgCCD4.1 expression in *E. coli* cells producing β-carotene as substrate reduced the quantity of the available substrate and rendered the production of crocetin dialdehyde, as detected by HPLC-MS system alongside authentical standard for the confirmation of the identity of the cleavage product.
(d) Induction of VgCCD4.1 expression in *E. coli* cells producing β-carotene as substrate reduced the quantity of the available substrate as observed by HPLC-MS.

regarding the presence of two longer β-strands in BdCCD4.1, which was due to the presence of additional amino acid residues located in positions 484–487 and changes in flanking amino acid residues (Figure S6d). The combined effect of multiple amino acid deletions and substitutions on protein function might thus be involved in

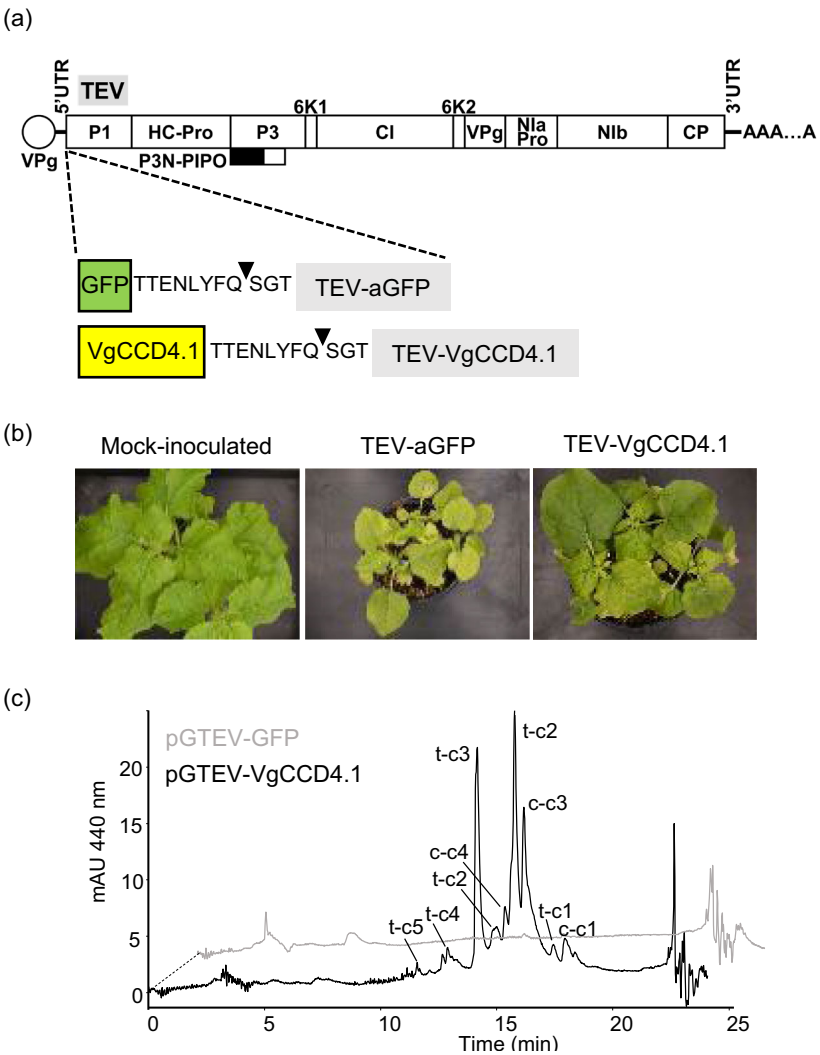

Figure 7. Inoculation of *N. benthamiana* plants that stably express NIb with TEV recombinant clones that express VgCCD4.1 and heterologous production of crocins.
(a) Schematic representation of TEV genome indicating the position where the GFP (green box) and the VgCCD4.1 (yellow box) were inserted. The sequence of the artificial NIaPro cleavage site to mediate the release of the recombinant proteins from the viral polyprotein is also indicated. The black triangle indicates the exact cleavage site. Lines represent TEV 5′ and 3′ UTR and boxes represent P1, HC-Pro, P3, P3N-PIPO, 6 K1, CI, 6 K2, VPg, NIaPro, NIb, and CP cistrons, as indicated.
(b) Pictures of representative leaves from plants mock-inoculated and agroinoculated with TEV-aGFP, and TEV-VgCCD4.1, as indicated, taken at 14 dpi. Scale bars correspond to 5 mm.
(c) Chromatographic profile at 440 nm of the polar fraction of leaves infected with TEV-aGFP, and TEV-VgCCD4.1. Peaks abbreviations correspond to: c-c1, cis-crocin 1; t-c1, trans-crocin 1; t-c2, trans-crocin 2; t-c2′, trans-crocin 2′; c-c3, cis-crocin 3, t-cr3, trans-crocin 3; c-c4, cis-crocin 4; t-c4, trans-crocin 4; t-c5, trans-crocetin 5.

long-range interactions in loops, helices, and β-strands that gate the substrate access channel, allowing the catalysis of different substrates (Acevedo-Rocha et al., 2021). Subsequently, the tridimensional structures of VgCCD4.1 and VsCCD4.1 were further overlapped with GjCCD4a, which recognizes zeaxanthin and β-carotene as substrates and has a 7,8:7′,8′ activity (Xu et al., 2020). GjCCD4a showed 56% and 52.6% identity with BdCCD4.1 and VgCCD4.1, respectively. In this case, the three structures displayed a major degree of overlapping (Figure S6c), suggesting that differences at the substrate level can be determined by changes at the structural level, which can influence multiple substrate-enzyme interaction points. In addition, the three proteins were analyzed for the residues involved in the interaction with the ligand 8-apo-β-carotenol (Figures S3 and S6c). Of interest, all the residues involved were identical among the three enzymes, except for one alanine residue in position 316 in the sequences of VgCCD4.1 and VsCCD4.1, which in BdCCD4.1 is substituted by proline (position 320). However, the presence of proline instead of alanine is also present at the same position in the enzyme of GjCCD4a (position 354). This amino acid is present as well in the enzyme from *Bixa orellana* BoCCD4.3 (position 298), which showed 7,8:7′,8′ activity on lycopene, β-carotene, and zeaxanthin (Frusciante et al., 2022). Although GjCCD4a and BoCCD4.3 show the same activity, their identity is less than 50% (48%) (Figure S7a), but overall, they showed very similar tridimensional structures (Figure S7b–d).

Next, we determined all the different residues present among the VgCCD4.1, VsCCD4.1, and BdCCD4.1 sequences, excluding differences in the predicted signal peptide (Figure S6c). Overall, a total of 30 differences were recorded, with more than 20 of them localized in the last 200 amino acids. These residues were compared with those present in the same positions in GjCCD4a and BoCCD4.3, as references for substrate recognition (Figure S7). A total of 18 residues were found to differ from

BdCCD4.1 and the other 4 CCDs (VgCCD4.1, VsCCD4.1, BoCCD4.3, and GjCCD4a) (Figure S8), which may be related to VgCCD4.1's ability to accept a wider variety of substrates. Finally, we investigated the affinity of VgCCD4.1 for β-carotene and zeaxanthin, yielding ΔG^0 values of −9.82 and − 8.32 Kcal/mol, respectively, while GjCCD4a displayed affinity values of −10.35 and − 9.81 Kcal/mol for each carotenoid substrate. In both cases, affinity values were higher for β-carotene than for zeaxanthin, suggesting that β-carotene is a better substrate for both enzymes.

DISCUSSION

Crocins are key bioactive metabolites that dissolve easily in water and produce a distinctive yellow color. Several studies have demonstrated that crocins possess antioxidant, radical quenching, and anti-inflammatory properties, which allow crocins to protect against oxidative damage to brain vasculature, the heart, renal tissues, and the retina, among other tissues (Cerdá-Bernad et al., 2022). Besides their anti-inflammatory and antioxidant properties, crocins exhibit anticancer activities, and have a potential against various malignant diseases, i.e., diabetes, Alzheimer's disease, and other chronic illnesses (Akhondzadeh et al., 2010; Wang et al., 2019). The main natural source of crocins is saffron, whose dry stigma is used as a spice, as well as an important ingredient for so-called functional food and beverages (Maqbool et al., 2022). In addition to crocins, the apocarotenoid picrocrocin, which also displays many interesting medicinal properties (Abu-Izneid et al., 2022), is also present in saffron. Although gardenia fruits have also been utilized in China as a source of crocins and as pigments, picrocrocin is not present in the fruits of this plant (Carmona et al., 2006).

In this work, we determine the levels of crocins and picrocrocin in the petals of *V. sinuatum* and *V. giganteum* and compare the profiles of crocins with the ones present in the stigma of *C. sativus* and in the corolla of *B. davidii*. The profiles of crocins in *Verbascum* were very similar to those in saffron, although the total levels of crocins were lower (9.81 mg/g for *V. giganteum* and 14.38 mg/g DW for *V. sinuatum*) compared to those in saffron, which fluctuated between 169 and 317 mg/g DW, depending on the country of origin (Anastasaki et al., 2010). In any case, the obtained levels were in the range of those observed in gardenia, from 10.08 to 36.97 mg/g DW (Thuy et al., 2022). These results reveal that *Verbascum* flowers are a source of crocins with enormous potential in several industrial fields.

Based on the previously characterized genes from *Buddleja*, encoding the enzymes catalyzing the biosynthesis of crocetin, we identified new *CCD* genes expressed in the petals of these two *Verbascum* species. A *CCD1* and three *CCD4* genes were identified in each species and their expression levels were analyzed in pre-anthesis and anthesis flowers. In both developmental stages and in both species, *CCD4.1* showed the higher expression levels; and its activity was further characterized. Two independent approaches were used to test the activity of this enzyme. VgCCD4.1 specifically catalyzed the cleavage of β-carotene and zeaxanthin at 7,8;7′,8′ double bonds when assayed in bacteria, producing crocetin dialdehyde, but does not cleave lycopene, indicating a requirement for a β-ring at the proximal end of the molecule. In addition, the activity of VgCCD4.1 (95.1% identity to VsCCD4.1) was tested in *N. benthamiana* plants using a TEV vector. This last approach was previously utilized to transiently overexpress the saffron enzyme, CsCCD2L, and the enzyme BdCCD4.1, from *B. davidii*, which resulted in the synthesis of crocins at 0.21% and 0.076% of leaf dry weight, respectively. These two enzymes only recognized zeaxanthin as substrate (Ahrazem et al., 2017; Frusciante et al., 2014; Zheng et al., 2022), which can limit their use to tissues where this carotenoid is present. The virus-based expression of VgCCD4.1 leads to crocin accumulation at 0.17% of leaf dry weight, demonstrating how this enzyme is a useful tool for producing crocins for industrial uses in a heterologous system such as *N. benthamiana*. Thus, the reaction catalyzed by the CCD4.1 enzymes from *Verbascum* expands the range of enzymes involved in crocins biosynthesis in dicotyledonous plants using different carotenoid substrates, which all belong to the CCD4 subfamily, as previously shown for Buddleja (Ahrazem et al., 2017) and gardenia enzymes (Xu et al., 2020). All the identified enzymes in *Verbascum sp*, CCD4.1, CCD4.2, and CCD4.3 are closely related to those from *B. davidii*. Interestingly, CCD4.1 and CCD4.3 are present in a specific sub-cluster, suggesting that the ancestor of these orthologs occurred before the split of *Verbascum* and *Buddleja*. Thus, it is most likely that the 7,8;7′,8′ activity evolved before this separation. However, we found differences at the level of substrate recognition, which might be associated with the observed alterations in the amino acid sequence. While the identity found among the CCD4.2 enzymes from *Buddleja* and *Verbascum* was relatively high (over 85%), CCD4.1 and CCD4.3 enzymes from *Verbascum* and *Buddleja* showed over 75% identity to each other. This suggests a higher divergence among the sequences of these two species, which may be related to the differences in substrate recognition observed between the CCD4.1 enzymes from *Verbascum* and *Buddleja*. In fact, a total of 29 amino acids were different, and an insertion of 4 amino acids was present in BdCCD4.1. These differences may be contributing to the observed substrate specificity, either individually or more probably through differential interactions among these residues as observed in other enzymes from the secondary metabolism in plants (Acevedo-Rocha et al., 2021), but also in CCD enzymes (Daruwalla et al., 2020; Sui et al., 2016) where mutagenic and structural analyses support the idea that

selectivity is similarly determined by multiple substrate-enzyme interaction points.

CONCLUSIONS

In this study, we characterized the crocin and picrocrocin derivatives produced and accumulated in the yellow flowers of two species of *Verbascum*, expanding the number of plant species that are able to produce and accumulate these important secondary metabolites. The enzymes implicated in the biosynthesis of these apocarotenoids in these species belong to the CCD4 sub-family, which include the enzymes initially identified in *Buddleja*, suggesting the specialization of these enzymes before the separation of these two species from the *Scrophulariaceae* family. Interestingly, the CCD enzyme from *Verbascum* recognized both β-carotene and zeaxanthin as substrates for cleavage. Because β-carotene is typically present at much higher levels than zeaxanthin in plant tissues, this broader specificity is crucial for the production of crocins in other heterologous systems and broadens the range of plants that could be engineered as hosts to produce these bioactive substances.

EXPERIMENTAL PROCEDURES

Collection of plant tissues from *Verbascum* sp

Flowers were collected from plants growing in the Botanical Garden of Castilla-La Mancha, Albacete, Spain. Care was taken to remove the anthers and other non-carotenoid-containing portions of the flower by trimming them away with scissors. Immediately after collection, the tissues were frozen at −80°C and stored until further use.

Extraction and analysis of carotenoids and apocarotenoids by HPLC-DAD

Tissues were ground in liquid nitrogen with a mixer mill MM400 (Retsch GmbH, Haan, Germany) in a 2 ml Eppendorf tube. Extraction was performed as previously described (Martí et al., 2020). In brief, 50% methanol was added to the homogenate, and the mix vortexed, sonicated, and centrifuged to recover polar metabolites. The pellet was extracted with 2:1 methanol:chloroform, mixed for an additional 10 min followed by centrifugation. The apolar phase was evaporated under N_2 gas and the dried residues were stored with the polar extracts at −80°C until analysis by HPLC. All assays were performed in triplicate.

The HPLC-DAD and HPLC-DAD-HRMS methods used for the analysis and detection of crocins, and carotenoids have been previously described (Diretto et al., 2019; Martí et al., 2020). Metabolite identification was done by comparison of retention times, UV–visible spectra, and MS data of authentic standards.

Nucleic acid purification and cDNA isolation

RNA was extracted from 100 mg of the frozen tissues by using Ambion PolyAtrack, following the manufacturer's protocols (Ambion Inc., Austin, TX, USA). First-strand cDNA was synthesized by reverse transcription (RT) from 1 μg of RNA using an 18-nucleotide oligo dT primer and a first-strand cDNA synthesis kit (GE Healthcare Life Sciences, Buckinghamshire, UK) according to the manufacturer's instructions. The synthesized cDNA was stored at −80°C.

PCR amplification and gene isolation

Sequence information was used to design specific primers for the isolation and cloning of the *CCD* genes (Supplementary Table S1). Synthesized cDNAs were used as templates for PCR using specific primers for each *CCD* gene (Supplementary Table S1). Thermal cycling parameters were 2 min at 95 °C, 35× (20 sec at 95 °C, 20 sec at 60°C and 2 min 30 sec at 72°C), and a final extension of 5 min at 72°C. The PCR products were ligated into pSpark-TA (Canvax, Cordoba, Spain) and used for *Escherichia coli* transformation by electroporation.

DNA sequencing and analysis of DNA and protein sequences

The obtained positive clones were sequenced using an automated DNA sequencer (ABI PRISM 3730xl, Perkin Elmer, Macrogen Inc., Seoul, Korea). Similarity searches were done with BLAST (NCBI; http://www.ncbi.nlm.nih.gov). *In silico* localization, analysis was carried out with the Plant Subcellular Localization Predictor (http://bioinfo.usu.edu/Plant-mSubP). The proteins were modeled using Phyre (http://www.sbg.bio.ic.ac.uk/phyre2) and Chimera X (https://www.cgl.ucsf.edu/chimerax/). Determination of substrate-affinity values, ΔG^0, was performed using MTiautoDock (https://bioserv.rpbs.univ-paris-diderot.fr/services/MTiOpenScreen/).

Phylogenetic analysis

The amino acid sequences were aligned using the BLOSUM62 matrix with the ClustalW (http://www.clustal.org) algorithm-based AlignX module from MEGA Version 11.0 (http://www.megasoftware.net/mega.htmL). The alignments were saved and executed by MEGA Version 11.0 to generate a Neighbor Joining Tree with bootstrapping (2500 replicates) analysis and handling gaps with pairwise deletion.

Gene expression by reverse transcription-quantitative PCR (RT-qPCR)

Total RNA was isolated from leaves and flowers at two developmental stages (pre-anthesis and anthesis) by grinding fresh tissues in liquid N_2 to a fine powder followed by Trizol reagent extraction (Gibco-BRL). The purified RNA was re-suspended in 100 μl of RNase-free water and treated with RQ1 RNase-free DNase (Promega, Madison, WI, USA). First-strand cDNAs were synthesized using a first-strand cDNA synthesis kit GE Healthcare Life Sciences (Buckinghamshire, UK) and Oligo-dT (18 mer) using 1 μg of total RNA. The obtained cDNA was used for RT-qPCR, using three biological replicates and specific primers (Supplemental Table S1); reactions were set up in a final volume of 25 μl in GoTaq® qPCR Master Mix (Promega, Madison, WI, USA) according to manufacturer's instructions. The housekeeping gene *Actin* served as a reference gene (Supplementary Table S1). The cycling parameters of qPCR consisted of an initial denaturation at 94°C for 5 min; 40 subsequent cycles of denaturation at 94°C for 20 sec, annealing at 58°C for 20 sec, and extension at 72°C for 20 sec; and finally, extension at 72°C for 5 min. Assays were conducted with a StepOne™ Thermal Cycler (Applied Biosystems, Foster City, California, USA). To ensure the reproducibility of the experiment, each sample was run in triplicate and analyzed using StepOne software v2.0 (Applied Biosystems, Foster City, California, USA).

Activity assays in E. Coli cells

Full-length cDNA was cloned into the *Eco*RI site of the pThio-Dan1 vector by recombination using the In-Fusion® HD Cloning Plus CE kit (Clontech, Saint-Germain-en-Laye, France) and specific primers (Supplementary Table S1). The resulting expression plasmid, named pThio-VgCCD4.1, was sequenced to confirm the correct assembly and sequence. The construct was used to transform *E. coli* BL21 containing the plasmids PAC-ZEAX, PAC-LYC, and PAC-BETA (https://www.addgene.org) to produce zeaxanthin, lycopene, and β-carotene. The transformants were cultured overnight at 30 °C in 4 mL 2YT medium supplemented with ampicillin (100 μg mL^{-1}) and chloramphenicol (60 μg mL^{-1}). The cultured cells were transferred to 50 ml 2xYT medium supplemented with ampicillin (50 μg mL^{-1}) and chloramphenicol (30 μg mL^{-1}) and further cultured at 30 °C until an OD600 of 0.8 was reached. Cells were then induced with 2% arabinose and grew overnight at 20°C. For HPLC analysis of the obtained products, the cells were harvested by centrifugation (11 000 ***g*** for 10 min) and pigments were extracted repeatedly in a total volume of 10 ml of acetone until all pigments were visibly removed. The solvent was evaporated under N_2 and the pigments resuspended with 0.5 ml of tert-methyl-butyl-ether. The extracts were analyzed as previously described (Ahrazem et al., 2022). All solvents used were HPLC-MS grade (Merck Millipore, Darmstadt, Germany). For GC-MS analyses, once the cells were induced, a total of 20 ml were transferred to special vials for volatile collection as previously described (Morote et al., 2023).

Activity assays in *N. benthamiana*

Plasmids were constructed by PCR amplification of cDNA of *VgCCD4.1* (Supplementary Table S1) and Gibson DNA assembly. The resulting plasmid contains a wild-type TEV cDNA (GenBank DQ986288, with two silent and neutral mutations G273A and A1119G) flanked by the CaMV 35S promoter and terminator in a binary vector derived from pCLEAN-G181 (Martí et al., 2020). The plasmid to express the recombinant TEVΔNIb-aGFP clone was previously described (Martí et al., 2020).

A. tumefaciens C58C1 competent cells, previously transformed with the helper plasmid pCLEAN-S48, were electroporated with the plasmid TEV-VgCCD4.1 and selected in plates with 50 μg/ml kanamycin, 50 μg/ml rifampicin, and 7.5 μg/ml tetracycline. Liquid cultures of selected colonies were prepared to infiltrate one leaf of one-month-old transgenic *N. benthamiana* that stably expresses TEV NIb. After infiltration, plants were kept under controlled conditions in a growth chamber at 25°C under a 12 h - day-night photoperiod. Leaf tissue was collected 14 days after infection (dpi) and analyzed for apocarotenoids and carotenoids content.

ACKNOWLEDGEMENTS

This work was supported by grant SBPLY/21/180225/000001 from Junta de Comunidades de Castilla-La Mancha, and PID2020-114761RB-I00 and PID2020-114691RB-I00 from the Ministerio de Ciencia e Innovación (Spain) through the Agencia Estatal de Investigación. LGG is a participant of the CARNET network (RED2022-134577-T).

AUTHOR CONTRIBUTIONS

Conceptualization: OA and LGG; writing, reviewing, and editing: LGG, OA, J-AD, and GD; plasmids construction, LM and VA; plant agroinfiltration, VA; expression analyses, LGG and A-JLJ; metabolite extraction and analyses, LGG, IM, GD, SF, and OD; activity assays, LM, AR-M, GD, and OD. All the authors read and approved the manuscript.

CONFLICT OF INTEREST

The authors declare no competing interest.

DATA AVAILABILITY STATEMENT

The data supporting our findings are available in the manuscript file or from the corresponding author upon request.

SUPPORTING INFORMATION

Additional Supporting Information may be found in the online version of this article.

Figure S1. Crocins profiles in *Verbascum* species, *Buddleja davidii*, and *Crocus sativus*. (a) Extracted ion chromatograms of m/z 329.17, from polar extracts of *C. sativus*, *V. giganteum*, and *V. sinuatum*. (b) HPLC-DAD/UV isoplot chromatograms of polar extracts of *V. sinuatum*, *V. giganteum*, *B. davidii*, and *C. sativus*.

Figure S2. HPLC chromatogram profiles of apolar extracts of flowers of *Verbascum sinuatum* (a) and *V. giganteum* (b).

Figure S3. Tridimensional structures of CCD4 enzymes. The green-colored structures represent the iron and substrate 8-apo-β-carotenol, in the left and right views of each CCD4, respectively. COACH was used to visualize the disposition of iron and the substrate.

Figure S4. Amino acid sequence alignment of VsCCD4.1 and VgCCD4.1 enzymes. Conserved amino acid residues are depicted with an asterisk.

Figure S5. Relative quantities of carotenoids (a) and chlorophylls (b) detected by HPLC-DAD in tissues of mock-inoculated and infected (TEV-aGFP, and TEV-VgCCD4.1) *N. benthamiana* plants. Data are averages ± SD of three biological replicates. Analyses were performed at 14 dpi.

Figure S6. Structurally optimized superposition of the model structures of CCDs showing the best geometries. (a) Superposition of VsCCD4.1 and VgCCD4.1. (b) Superposition of VsCCD4.1, VgCCD4.1 and BdCCD4.1. (c) Superposition of VsCCD4.1, VgCCD4.1 and GjCCd4a. Models were obtained by using Chimera (https://www.cgl.ucsf.edu/chimerax/). (d) Amino acid sequence alignment of BdCCD4.1, VgCCD4.1, and VsCCD4.1. Conserved amino acid residues are depicted with asterisk. The amino acid residues involved in iron coordination are highlighted in yellow and blue, in green the conserved His residues. In red are labeled the residues not conserved between the *Verbascum* and *Buddleja* enzymes.

Figure S7. Comparative analyses between GjCCD4a and BoCCD4.3. (a) Amino acid sequence alignment of BoCCD4.3, and GjCCD4a. Conserved amino acid residues are depicted with asterisk. Identity between these two enzymes is 48%. Tridimensional structures (b and c) and structurally optimized superposition of the model structures of GjCCD4a and BoCCD4.3. Models were obtained by using Chimera (https://www.cgl.ucsf.edu/chimerax/).

Figure S8. Amino acid sequence alignment of BoCCd4.3, GjCCD4a, BdCCD4.1, VgCCD4.1 and VsCCD4.1. Conserved amino acid residues are depicted with asterisk. The black arrows depicted the amino acid residues that differ with respect to BdCCD4.1 in VsCCD4.1, VgCCD4.1 and GjCCD4a and BoCCD4.3.

Table S1. Oligonucleotide sequences used for cloning, expression, and activity assays.

REFERENCES

Abu-Izneid, T., **Rauf, A.**, **Khalil, A.A.**, **Olatunde, A.**, **Khalid, A.**, **Alhumaydhi, F.A.** ***et al.*** (2022) Nutritional and health beneficial properties of saffron (Crocus sativus L): a comprehensive review. *Critical Reviews in Food Science and Nutrition*, **62**, 2683–2706.

Acevedo-Rocha, C.G., **Li, A.**, **D'Amore, L.**, **Hoebenreich, S.**, **Sanchis, J.**, **Lubrano, P.** ***et al.*** (2021) Pervasive cooperative mutational effects on multiple catalytic enzyme traits emerge via long-range conformational dynamics. *Nature Communications*, **12**, 1621.

Ahrazem, O., **Diretto, G.**, **Argandona, J.**, **Rubio-Moraga, A.**, **Julve, J.M.**, **Orzaez, D.** ***et al.*** (2017) Evolutionarily distinct carotenoid cleavage dioxygenases are responsible for crocetin production in Buddleja davidii. *Journal of Experimental Botany*, **68**, 14–4677.

Ahrazem, O., **Diretto, G.**, **Rambla, J.L.**, **Rubio-Moraga, Á.**, **Lobato-Gómez, M.**, **Frusciante, S.** ***et al.*** (2022) Engineering high levels of saffron apocarotenoids in tomato. *Horticulture Research*, **9**, uhac074.

Ahrazem, O., **Gomez-Gomez, L.**, **Rodrigo, M.J.**, **Avalos, J.** & **Limon, M.C.** (2016) Carotenoid cleavage Oxygenases from microbes and photosynthetic organisms: features and functions. *International Journal of Molecular Sciences*, **17**, 1781. Available from: https://doi.org/10.3390/ijms17111781

Ahrazem, O., **Rubio-Moraga, A.**, **Berman, J.**, **Capell, T.**, **Christou, P.**, **Zhu, C.** ***et al.*** (2016) The carotenoid cleavage dioxygenase CCD2 catalysing the synthesis of crocetin in spring crocuses and saffron is a plastidial enzyme. *New Phytologist*, **209**, 13–663.

Akhondzadeh, S., **Sabet, M.S.**, **Harirchian, M.H.**, **Togha, M.**, **Cheraghmakani, H.**, **Razeghi, S.** ***et al.*** (2010) Saffron in the treatment of patients with mild to moderate Alzheimer's disease: a 16-week, randomized and placebo-controlled trial. *Journal of Clinical Pharmacy and Therapeutics*, **35**, 581–588.

Alder, A., **Holdermann, I.**, **Beyer, P.** & **Al-Babili, S.** (2008) Carotenoid oxygenases involved in plant branching catalyse a highly specific conserved apocarotenoid cleavage reaction. *The Biochemical Journal*, **416**, 289–296.

Alder, A., **Jamil, M.**, **Marzorati, M.**, **Bruno, M.**, **Vermathen, M.**, **Bigler, P.** ***et al.*** (2012) The path from beta-carotene to carlactone, a strigolactone-like plant hormone. *Science*, **335**, 1348–1351.

Anastasaki, E.G., **Kanakis, C.D.**, **Pappas, C.**, **Maggi, L.**, **Zalacain, A.**, **Carmona, M.** ***et al.*** (2010) Quantification of crocetin esters in saffron (Crocus sativus L.) using Raman spectroscopy and chemometrics. *Journal of Agricultural and Food Chemistry*, **58**, 6011–6017.

Auldridge, M.E., **Block, A.**, **Vogel, J.T.**, **Dabney-Smith, C.**, **Mila, I.**, **Bouzayen, M.** ***et al.*** (2006) Characterization of three members of the Arabidopsis carotenoid cleavage dioxygenase family demonstrates the divergent roles of this multifunctional enzyme family. *The Plant Journal*, **45**, 982–993.

Auldridge, M.E., **McCarty, D.R.** & **Klee, H.J.** (2006) Plant carotenoid cleavage oxygenases and their apocarotenoid products. *Current Opinion in Plant Biology*, **9**, 315–321.

Awasthi, P., **Khan, S.**, **Lakhani, H.**, **Chaturvedi, S.S.**, **Kaur, N.**, **Singh, J.** ***et al.*** (2022) Transgene-free genome editing supports the role of carotenoid cleavage dioxygenase 4 as a negative regulator of β-carotene in banana. *Journal of Experimental Botany*, **73**, 3401–3416.

Bate-Smith, E.C. (1953) Colour reactions of flowers attributed to (a) flavanols and (b) carotenoid oxides. *Journal of Experimental Botany*, **4**, 9.

Benedí, C. (2009) Verbascum. In: Benedí Gonzalez, C.R.H.E., Güemes Heras, J. & Herrero Nieto, A. (Eds.) *Flora Iberica*. Madrid, Spain: CSIC, pp. 49–97.

Blanco-Salas, J., **Hortigón-Vinagre, M.P.**, **Morales-Jadán, D.** & **Ruiz-Téllez, T.** (2021) Searching for scientific explanations for the uses of Spanish folk medicine: a review on the case of mullein (*Verbascum*, Scrophulariaceae). *Biology (Basel)*, **10**, 618.

Brandi, F., **Bar, E.**, **Mourgues, F.**, **Horvath, G.**, **Turcsi, E.**, **Giuliano, G.** ***et al.*** (2011) Study of 'Redhaven' peach and its white-fleshed mutant suggests a key role of CCD4 carotenoid dioxygenase in carotenoid and norisoprenoid volatile metabolism. *BMC Plant Biology*, **11**, 24.

Bruno, M., **Beyer, P.** & **Al-Babili, S.** (2015) The potato carotenoid cleavage dioxygenase 4 catalyzes a single cleavage of beta-ionone ring-containing carotenes and non-epoxidated xanthophylls. *Archives of Biochemistry and Biophysics*, **572**, 126–133.

Bruno, M., **Hofmann, M.**, **Vermathen, M.**, **Alder, A.**, **Beyer, P.** & **Al-Babili, S.** (2014) On the substrate- and stereospecificity of the plant carotenoid cleavage dioxygenase 7. *FEBS Letters*, **588**, 1802–1807.

Carmona, M., **Zalacain, A.**, **Sanchez, A.M.**, **Novella, J.L.** & **Alonso, G.L.** (2006) Crocetin esters, picrocrocin and its related compounds present in Crocus sativus stigmas and Gardenia jasminoides fruits. Tentative identification of seven new compounds by LC-ESI-MS. *Journal of Agricultural and Food Chemistry*, **54**, 973–979.

Cerdá-Bernad, D., **Valero-Cases, E.**, **Pastor, J.J.** & **Frutos, M.J.** (2022) Saffron bioactives crocin, crocetin and safranal: effect on oxidative stress and mechanisms of action. *Critical Reviews in Food Science and Nutrition*, **62**, 3232–3249.

Daruwalla, A., **Zhang, J.**, **Lee, H.J.**, **Khadka, N.**, **Farquhar, E.R.**, **Shi, W.** ***et al.*** (2020) Structural basis for carotenoid cleavage by an archaeal carotenoid dioxygenase. *Proceedings of the National Academy of Sciences of the United States of America*, **117**, 19914–19925.

Diretto, G., **Ahrazem, O.**, **Rubio-Moraga, A.**, **Fiore, A.**, **Sevi, F.**, **Argandona, J.** ***et al.*** (2019) UGT709G1: a novel uridine diphosphate glycosyltransferase involved in the biosynthesis of picrocrocin, the precursor of safranal in saffron (Crocus sativus). *The New Phytologist*, **224**, 725–740.

Dong, X., **Mkala, E.M.**, **Mutinda, E.S.**, **Yang, J.X.**, **Wanga, V.O.**, **Oulo, M.A.** ***et al.*** (2022) Taxonomy, comparative genomics of mullein (Verbascum, Scrophulariaceae), with implications for the evolution of Verbascum and Lamiales. *BMC Genomics*, **23**, 566.

Frusciante, S., **Demurtas, O.C.**, **Sulli, M.**, **Mini, P.**, **Aprea, G.**, **Diretto, G.** ***et al.*** (2022) Heterologous expression of Bixa orellana cleavage dioxygenase 4-3 drives crocin but not bixin biosynthesis. *Plant Physiology*, **188**, 1469–1482.

Frusciante, S., **Diretto, G.**, **Bruno, M.**, **Ferrante, P.**, **Pietrella, M.**, **Prado-Cabrero, A.** ***et al.*** (2014) Novel carotenoid cleavage dioxygenase catalyzes the first dedicated step in saffron crocin biosynthesis. *Proceedings of the National Academy of Sciences of the United States of America*, **111**, 12246–12251.

Garcia-Limones, C., **Schnabele, K.**, **Blanco-Portales, R.**, **Luz Bellido, M.**, **Caballero, J.L.**, **Schwab, W.** ***et al.*** (2008) Functional characterization of FaCCD1: a carotenoid cleavage dioxygenase from strawberry involved in lutein degradation during fruit ripening. *Journal of Agricultural and Food Chemistry*, **56**, 9277–9285.

Gomez-Gomez, L., **Pacios, L.F.**, **Diaz-Perales, A.**, **Garrido-Arandia, M.**, **Argandona, J.**, **Rubio-Moraga, A.** ***et al.*** (2018) Expression and interaction analysis among saffron ALDHs and crocetin dialdehyde. *International Journal of Molecular Sciences*, **19**(5), 1409. Available from: https://doi.org/10.3390/ijms19051409

Gomez-Gomez, L., **Parra-Vega, V.**, **Rivas-Sendra, A.**, **Segui-Simarro, J.M.**, **Molina, R.V.**, **Pallotti, C.** ***et al.*** (2017) Unraveling massive Crocins transport and accumulation through proteome and microscopy tools during the development of saffron stigma. *International Journal of Molecular Sciences*, **18**(1), 76. Available from: https://doi.org/10.3390/ijms18010076

Gonzalez-Jorge, S., **Ha, S.H.**, **Magallanes-Lundback, M.**, **Gilliland, L.U.**, **Zhou, A.**, **Lipka, A.E.** ***et al.*** (2013) Carotenoid cleavage dioxygenase4 is a negative regulator of beta-carotene content in Arabidopsis seeds. *Plant Cell*, **25**, 4812–4826.

Huang, F.C., **Horvath, G.**, **Molnar, P.**, **Turcsi, E.**, **Deli, J.**, **Schrader, J.** ***et al.*** (2009) Substrate promiscuity of RdCCD1, a carotenoid cleavage oxygenase from Rosa damascena. *Phytochemistry*, **70**, 457–464.

Ibdah, M., **Azulay, Y.**, **Portnoy, V.**, **Wasserman, B.**, **Bar, E.**, **Meir, A.** ***et al.*** (2006) Functional characterization of CmCCD1, a carotenoid cleavage dioxygenase from melon. *Phytochemistry*, **67**, 1579–1589.

Ilg, A., **Bruno, M.**, **Beyer, P.** & **Al-Babili, S.** (2014) Tomato carotenoid cleavage dioxygenases 1A and 1B: relaxed double bond specificity leads to a plenitude of dialdehydes, mono-apocarotenoids and isoprenoid volatiles. *FEBS Open Bio*, **4**, 584–593.

Jan, F., **Jan, B.**, **Akbar Dar, M.**, **Sofi, F.A.**, **Alsuwayni, B.M.**, **Afzal, S.** ***et al.*** (2022) A review on traditional uses, phytochemistry, and pharmacological activities of Verbascum thapsus. In: Masoodi, M.H. & Rehman, M.U. (Eds.) *Edible Plants in Health and Diseases: Volume II: Phytochemical and Pharmacological Properties*. Singapore: Springer Singapore, pp. 483–500.

Kloer, D.P. & **Schulz, G.E.** (2006) Structural and biological aspects of carotenoid cleavage. *Cellular and Molecular Life Sciences*, **63**, 2291–2303.

López-Jimenez, A.J., **Frusciante, S.**, **Niza, E.**, **Ahrazem, O.**, **Rubio-Moraga, Á.**, **Diretto, G.** ***et al.*** (2021) A new glycosyltransferase enzyme from family 91, UGT91P3, is responsible for the final Glucosylation step of Crocins

in saffron (Crocus sativus L.). *International Journal of Molecular Sciences*, **22**(16), 8815. Available from: https://doi.org/10.3390/ijms22168815

Ma, G., **Zhang, L.**, **Matsuta, A.**, **Matsutani, K.**, **Yamawaki, K.**, **Yahata, M.** ***et al.*** (2013) Enzymatic formation of beta-Citraurin from beta-cryptoxanthin and zeaxanthin by carotenoid cleavage Dioxygenase4 in the flavedo of citrus fruit. *Plant Physiology*, **163**, 682–695.

Maoka, T. (2021) Carotenoid Metabolism in Terrestrial Animals. In: Misawa, N. (Ed.) *Carotenoids: Biosynthetic and biofunctional approaches*. Springer Singapore: Singapore, pp. 51–66.

Maqbool, Z., **Arshad, M.S.**, **Ali, A.**, **Aziz, A.**, **Khalid, W.**, **Afzal, M.F.** ***et al.*** (2022) Potential role of phytochemical extract from saffron in development of functional foods and protection of brain-related disorders. *Oxidative Medicine and Cellular Longevity*, **2022**, 6480590.

Martí, M., **Diretto, G.**, **Aragonés, V.**, **Frusciante, S.**, **Ahrazem, O.**, **Gómez-Gómez, L.** ***et al.*** (2020) Efficient production of saffron crocins and picrocrocin in Nicotiana benthamiana using a virus-driven system. *Metabolic Engineering*, **61**, 238–250.

Moraga, A.R., **Nohales, P.F.**, **Perez, J.A.** & **Gomez-Gomez, L.** (2004) Glucosylation of the saffron apocarotenoid crocetin by a glucosyltransferase isolated from Crocus sativus stigmas. *Planta*, **219**, 955–966.

Morote, L., **Rubio-Moraga, Á.**, **López-Jiménez, A.J.**, **Argandoña, J.**, **Niza, E.**, **Ahrazem, O.** ***et al.*** (2023) A carotenoid cleavage dioxygenase 4 from Paulownia tomentosa determines visual and aroma signals in flowers. *Plant Science*, **329**, 111609.

Ohmiya, A., **Kishimoto, S.**, **Aida, R.**, **Yoshioka, S.** & **Sumitomo, K.** (2006) Carotenoid cleavage dioxygenase (CmCCD4a) contributes to white color formation in chrysanthemum petals. *Plant Physiology*, **142**, 1193–1201.

Pfander, H. & **Schurtenberger, H.** (1982) Biosynthesis of C20-carotenoids in crocus sativus. *Phytochemistry*, **21**, 4–1042.

Rodrigo, M.J., **Alquezar, B.**, **Alos, E.**, **Medina, V.**, **Carmona, L.**, **Bruno, M.** ***et al.*** (2013) A novel carotenoid cleavage activity involved in the biosynthesis of citrus fruit-specific apocarotenoid pigments. *Journal of Experimental Botany*, **64**, 4461–4478.

Rodriguez-Concepcion, M., **Avalos, J.**, **Bonet, M.L.**, **Boronat, A.**, **Gomez-Gomez, L.**, **Hornero-Mendez, D.** ***et al.*** (2018) A global perspective on carotenoids: metabolism, biotechnology, and benefits for nutrition and health. *Progress in Lipid Research*, **70**, 62–93.

Rubio, A., **Rambla, J.L.**, **Santaella, M.**, **Gomez, M.D.**, **Orzaez, D.**, **Granell, A.** ***et al.*** (2008) Cytosolic and plastoglobule-targeted carotenoid dioxygenases from Crocus sativus are both involved in beta-ionone release. *The Journal of Biological Chemistry*, **283**, 24816–24825.

Rubio-Moraga, A., **Rambla, J.L.**, **Fernandez-de-Carmen, A.**, **Trapero-Mozos, A.**, **Ahrazem, O.**, **Orzaez, D.** ***et al.*** (2014) New target carotenoids for CCD4 enzymes are revealed with the characterization of a novel stress-induced carotenoid cleavage dioxygenase gene from Crocus sativus. *Plant Molecular Biology*, **86**, 555–569.

Salih, N.A., **Nadhaif, E.T.** & **Hussein, R.A.** (2019) Bioactivity of crocin pigment of saffron plant. *Plant Archives*, **18**(1), 357.

Schmidt, H., **Kurtzer, R.**, **Eisenreich, W.** & **Schwab, W.** (2006) The carotenase AtCCD1 from Arabidopsis thaliana is a dioxygenase. *The Journal of Biological Chemistry*, **281**, 9845–9851.

Schwartz, S.H., **Tan, B.C.**, **Gage, D.A.**, **Zeevaart, J.A.** & **McCarty, D.R.** (1997) Specific oxidative cleavage of carotenoids by VP14 of maize. *Science*, **276**, 1872–1874.

Schwartz, S.H., **Tan, B.C.**, **McCarty, D.R.**, **Welch, W.** & **Zeevaart, J.A.** (2003) Substrate specificity and kinetics for VP14, a carotenoid cleavage dioxygenase in the ABA biosynthetic pathway. *Biochimica et Biophysica Acta*, **1619**, 9–14.

Simkin, A.J. (2021) Carotenoids and apocarotenoids in planta: their role in plant development, contribution to the flavour and aroma of fruits and flowers, and their nutraceutical benefits. *Plants (Basel)*, **10**, 2321.

Simkin, A.J., **Underwood, B.A.**, **Auldridge, M.**, **Loucas, H.M.**, **Shibuya, K.**, **Schmelz, E.** ***et al.*** (2004) Circadian regulation of the PhCCD1 carotenoid cleavage dioxygenase controls emission of beta-ionone, a fragrance volatile of petunia flowers. *Plant Physiology*, **136**, 3504–3514.

Sui, X., **Zhang, J.**, **Golczak, M.**, **Palczewski, K.** & **Kiser, P.D.** (2016) Key residues for catalytic function and metal coordination in a carotenoid cleavage dioxygenase*. *Journal of Biological Chemistry*, **291**, 19401–19412.

Thuy, N.M., **Nhu, P.H.**, **Tai, N.V.** & **Minh, V.Q.** (2022) Extraction optimization of crocin from gardenia (Gardenia jasminoides Ellis)fruits using response surface methodology and quality evaluation of foam-mat dried powder. *Horticulturae*, **8**, 1199.

Wang, C., **Cai, X.**, **Hu, W.**, **Li, Z.**, **Kong, F.**, **Chen, X.** ***et al.*** (2019) Investigation of the neuroprotective effects of crocin via antioxidant activities in HT22 cells and in mice with Alzheimer's disease. *International Journal of Molecular Medicine*, **43**, 956–966.

Wang, J., **Zhang, N.**, **Zhao, M.**, **Jing, T.**, **Jin, J.**, **Wu, B.** ***et al.*** (2020) Carotenoid cleavage dioxygenase 4 catalyzes the formation of carotenoid-derived volatile β-ionone during tea (Camellia sinensis) withering. *Journal of Agricultural and Food Chemistry*, **68**, 1684–1690.

Xu, Z., **Pu, X.**, **Gao, R.**, **Demurtas, O.C.**, **Fleck, S.J.**, **Richter, M.** ***et al.*** (2020) Tandem gene duplications drive divergent evolution of caffeine and crocin biosynthetic pathways in plants. *BMC Biology*, **18**, 63.

Zhang, B., **Liu, C.**, **Wang, Y.**, **Yao, X.**, **Wang, F.**, **Wu, J.** ***et al.*** (2015) Disruption of a CAROTENOID CLEAVAGE DIOXYGENASE 4 gene converts flower colour from white to yellow in brassica species. *The New Phytologist*, **206**, 1513–1526.

Zhang, J., **He, L.**, **Dong, J.**, **Zhao, C.**, **Wang, Y.**, **Tang, R.** ***et al.*** (2023) Integrated metabolic and transcriptional analysis reveals the role of carotenoid cleavage dioxygenase 4 (IbCCD4) in carotenoid accumulation in sweetpotato tuberous roots. *Biotechnology for Biofuels and Bioproducts*, **16**, 45.

Zheng, X., **Mi, J.**, **Balakrishna, A.**, **Liew, K.X.**, **Ablazov, A.**, **Sougrat, R.** ***et al.*** (2022) Gardenia carotenoid cleavage dioxygenase 4a is an efficient tool for biotechnological production of crocins in green and non-green plant tissues. *Plant Biotechnology Journal*, **20**, 2202–2216.

Zhong, Y., **Pan, X.**, **Wang, R.**, **Xu, J.**, **Guo, J.**, **Yang, T.** ***et al.*** (2020) ZmCCD10a encodes a distinct type of carotenoid cleavage dioxygenase and enhances plant tolerance to low phosphate. *Plant Physiology*, **184**, 374–392.